Tonotopic Mapping in Inferior Colliculus using bSSFP fMRI and Sweeping Frequency Auditory Stimulation

M. M. Cheung[1,2], J. S. Cheng[1,2], I. Y. Zhou[1,2], K. C. Chan[1,2], C. Lau[1,2], and E. X. Wu[1,2]

[1]Laboratory of Biomedical Imaging and Signal Processing, The University of Hong Kong, Pokfulam, Hong Kong SAR, China, People's Republic of, [2]Department of Electrical and Electronic Engineering, The University of Hong Kong, Pokfulam, Hong Kong SAR, China, People's Republic of

INTRODUCTION The inferior colliculus (IC) is an important auditory relay center for ascending pathways and the central nucleus of IC (CIC) receives input from lower auditory centers and projects to the medial geniculate body in a strictly tonotopic manner [1]. To investigate such complex functional structures in development and disease models, an in vivo and non-invasive technique with high spatial resolution and fidelity is desired. Given the unique property that individual neurons are sensitive to different characteristic frequencies in IC [2], a novel periodic frequency-modulated auditory stimulus with linearly sweeping frequency was proposed for mapping the tonotopic organization in rat IC with fMRI. Tonotopic mapping was obtained based on the magnitude and phase information in Fourier transform of the time series. Furthermore, because the commonly used EPI sequences suffer from spatial distortions due to off-resonance effects and gradient eddy currents [3], we employed the balanced steady state free precession (bSSFP) fMRI approach that was recently proposed and demonstrated for distortion-free and potentially high resolution functional imaging [4,5]. We demonstrated in this study that the combination of bSSFP with periodic sweeping frequency stimulation could provide an efficient and robust tonotopic mapping in IC.

METHODS ***Animal preparation*** Normal male SD rats (n=4) were anesthetized using isoflurane (3% induction, 1.5% maintenance) and kept warm with 37^{0}C water throughout the experiment. Respiration rate, heart rate, SpO_2, end-tidal CO_2 level and rectal temperature were monitored. ***Auditory stimuli*** The stimuli were produced using a closed-field electrostatic loudspeaker (TDT EC1) driven by an amplifier (TDT ED1), and delivered to the rat ear canal via a flexible sound delivery tube (Tygon) of diameter 2mm and length 10cm. **(1)** Frequency-modulated (0.1mHz-40kHz) sweeping frequency with cyclic duration of 40s was delivered (Fig.1). **(2)** For comparison, pure tone bursts of 7, 20 and 40kHz were presented in a randomly interleaved order in a block-designed sequence consisting of 20s auditory stimulation, followed by 40s silence. ***MRI protocol*** MRI experiments were performed using a Bruker 7T scanner. Fieldmap-based shimming technique was applied prior to fMRI scans. 2D bSSFP image series of a single coronal slice covering the entire IC were acquired with TR/TE=3.8/1.9ms, FA=30^0, phase advance=180^0, FOV=32x32x120mm^3, data matrix=64x64 (zero-filled to 128x128), NEX=4 (temporal resolution=1s). ***Data analysis*** Data in the first 40s of each scan were discarded. The remaining fMRI time series were co-registered using AIR5.2.5 before further analysis. **(i)** Fourier transform of the fMRI time series were performed on a voxel-by-voxel basis to obtain magnitude and phase at the modulating frequency (0.025Hz=1/40s). The magnitude was arbitrarily normalized by the area under the entire spectral magnitude function. Voxels were considered as activated when the percentage of this fraction > $5x10^{-7}$ and cluster size>2. The activation delay (from 0.1mHz) at each individual voxel was then calculated by multiplying the phase with 40s/2π, from which the corresponding stimulation frequency was computed. **(ii)** 12-24 blocks of the same stimuli were averaged from multiple scans per stimulus frequency. The averaged time profiles were concatenated before statistical analysis using STIMULATE.

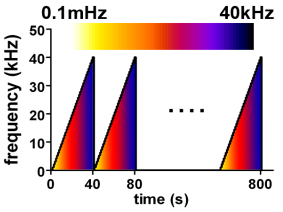

Fig.1 Stimulation paradigm: frequencies were swept in a cycle of 40s for 800s.

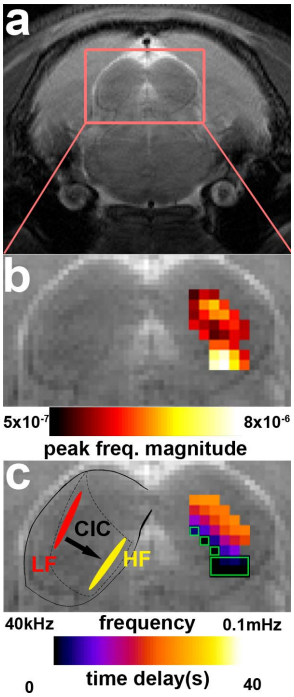

Fig.2 (a) Single coronal slice was scanned covering the entire IC. **(b)** Typical spectral magnitude at the modulating frequency (0.025Hz=1/40s). **(c)** (*Left*) Schematic diagram (adapted from Paxinos atlas) illustrating isofrequency bands of lower (LF) and higher (HF) characteristic frequency in the central nucleus of IC (CIC). (*Right*) Calibrated time delay (i.e., stimulation frequency) map computed from phase information at 0.025Hz. Note that delays have been corrected for hemodynamic delay using subtraction by the average phase within HF voxels marked in green (see Discussions).

RESULTS Fig.2 shows typical magnitude and time delay maps computed from the times series acquired using periodic sweeping frequency stimulus. The time delay map in Fig. 2c shows clear iso-delay bands aligned in excellent agreement with known neuroanatomy of IC [6]. Similar pattern of monotonically increasing delay along the medio-lateral direction were seen in all animals. Fig.3 shows the frequency tonotopic mapping of IC using block design stimulus. Activation by the 3 pure tone sounds could also be differentiated spatially but with poor quality. In addition, Fig.4 shows the BOLD activation and its changes (acquired using standard SE-EPI) vs. the power of acoustic stimulation, indicating an approximately linear monotonic dependency on stimulus (for which a separate abstract has been submitted with detailed elaborations).

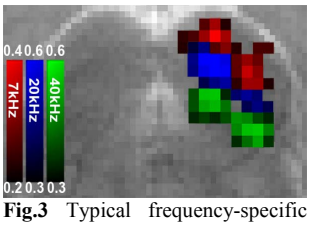

Fig.3 Typical frequency-specific tonotopic mapping of IC with correlation coefficient map overlaid on an anatomical image (red: 7kHz; blue: 20kHz; green: 40kHz).

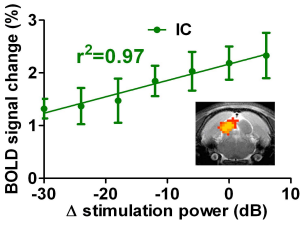

Fig.4 BOLD change vs. change of power (dB) of acoustic stimulation. Signal from IC show an approximately linearly increasing trend with stimulus power.

DISCUSSIONS and CONCLUSIONS In this study, a novel technique using bSSFP acquisition and sweeping frequency auditory stimulation has been proposed for tonotopic mapping in IC. Tonotopic information at each voxel was derived from the corresponding activation temporal delay that was computed from the phase information in Fourier transform of the time series for that voxel. This approach clearly yielded better tonotopic mapping than the block design approach (Fig. 2c vs. Fig. 3). Note that the activated voxels covering 20-40kHz in Fig.2b co-localized with the region activated by 20-40kHz in Fig. 3. These findings demonstrated that the proposed technique is robust and efficient for tonotopic mapping in IC while providing high spatial-specificity and sensitivity about the tonotopy. The continuous dispersion of different frequencies in Fig. 2c was consistent with known neuroanatomy studied by immunohistochemistry [6]. On the other hand, one challenge in fMRI study of auditory system is the presence of scanner noise. In Fig. 4, BOLD percentage change was approximately linear in the range of stimulus power applied, which paralleled the previous findings of neuronal activities by other methods [7]. Such linear relationship indicated that the observed BOLD activation can therefore be considered as the additional on/off activation that is superimposed on the elevated baseline activation by scanner noise. Note that the continuous scanner noise in bSSFP induces a more stable and smooth baseline activation, thus providing further advantage over EPI for auditory fMRI. In this study, the delays shown in Fig 2c were corrected for hemodynamic delay by subtraction of the average phase in the voxels marked by green boxes (which are known to be the high frequency region). However, such self-correction based on priori knowledge can be eliminated. For example, one can perform a separate experiment using short noise burst blocks but with period and repetition paradigm identical to Fig. 1, from which one can calculate the correction phase from the time series of activated voxels in IC using similar analysis, and correct for the hemodynamic delay. In summary, tonotopic mapping in IC by fMRI has been successfully demonstrated here for the first time in animals or humans.

REFERENCES 1. Lee CC et al, PNAS, 2010. 2. Pierson M et al, Brain Research, 1994. 3. Jezzard P et al. MRM 1995. 4. Scheffler K et al, NMR Biomed 2001. 5. Lee JH et al, Nature, 2010. 6. Malmierca MS et al, J Neurosci, 2008. 7. Polley DB et al, PNAS 2004.